Glycosaminoglycan Deposition in Engineered Cartilage: Experiments and Mathematical Model

Bojana Obradovic and Jerry H. Meldon
Dept. of Chemical and Biological Engineering, Tufts University, Medford, MA 02155

Lisa E. Freed and Gordana Vunjak-Novakovic
Division of Health Sciences and Technology, Massachusetts Institute of Technology, Cambridge, MA 02139

Functional cartilaginous constructs for scientific research and eventual tissue repair were cultivated in bioreactors starting from chondrocytes immobilized on polymeric scaffolds. The scaffolds gradually degraded as the cells regenerated tissue matrix consisting of glycosaminoglycan (GAG) and type II collagen. To facilitate data interpretation and optimize cultivation conditions, a mathematical model was developed which yields the concentrations of oxygen and GAG as functions of time and position in growing tissue. Calculated GAG concentrations were qualitatively and quantitatively consistent with profiles measured via high-resolution image processing of tissue samples cultured at two different oxygen tensions for various periods of time.

Introduction

More than one-million patients per year require treatment of damaged cartilage (Langer and Vacanti, 1993), a relatively simple structural tissue with one main function (load bearing) and very limited capacity for self-repair. However, none of the available treatment options can predictably restore a durable articular surface to an osteoarthritic or injured joint (Buckwalter and Mankin, 1998). *In vitro* tissue engineering has been investigated as a potential source of functional tissue constructs for cartilage repair, as well as a model system for controlled studies of cartilage development (chondrogenesis), and normal and pathological function (Freed and Vunjak-Novakovic, 2000a; Freed et al., 1999).

Cartilage constructs have been successfully grown in tissue culture bioreactors starting from chondrogenic cells attached to biodegradable polymeric scaffolds (Freed and Vunjak-Novakovic, 2000b; Vunjak-Novakovic et al., 1999). Improvements in construct composition, such as increased fractions of glycosaminoglycan (GAG) and collagen, the main cartilage components, were observed when either the scaffold thickness was decreased or the cell density was increased (Freed et al., 1994a). This apparently reflected diffusion-limited supply of nutrients and/or oxygen (Freed et al., 1994b; Bursac et al., 1996). More efficient gas transport in both the culture medium and at the construct surfaces stimulated rapid tissue growth, while cultivation at low oxygen tension suppressed chondrogenesis (Obradovic et al., 1999). Mixing during cell seeding and tissue cultivation resulted in both greater amounts and more uniform distributions of tissue components (Vunjak-Novakovic et al., 1996). Use of rotating bioreactors with dynamic laminar flow accelerated chondrogenesis, compared with either static culture, which yielded mechanically weak constructs with only peripheral matrix deposition, or unidirectional turbulent flow in mixed flasks, which yielded constructs with fibrous outer capsules (Vunjak-Novakovic et al., 1999).

In constructs cultured in bioreactors, tissue regeneration proceeded from the tissue periphery both outward and toward the construct center, and resulted in cartilaginous matrix comprised of glycosaminoglycan (GAG) and type II collagen (Freed et al., 1998). Cells proliferated over the first 5–7 days. Only after cell growth ceased did the cells begin to separate themselves by synthesizing matrix components. After 6 weeks of cultivation, the constructs' GAG wet weight fractions and equilibrium moduli, respectively, attained 78%

Correspondence concerning this article should be addressed to G. Vunjak-Novakovic.

and 25% of the values measured in freshly explanted native cartilage (Vunjak-Novakovic et al., 1999); after 7 months, the GAG fractions and equilibrium moduli of engineered and native cartilage were indistinguishable (Freed et al., 1997).

Construct function (such as mechanical behavior in static and dynamic compression) was correlated with overall construct composition, which itself depended on the conditions of bioreactor cultivation (Vunjak-Novakovic et al., 1999). Empirical relationships like these are fundamentally instructive. However, the spatial averaging intrinsic to measurement of overall construct properties filters out potentially significant information regarding internal gradients and associated mass-transfer limitations upon cell metabolism and/or tissue growth. Furthermore, global property data does not provide a severe test of distributed-parameter models of cartilage growth.

To simulate cell proliferation in cell-polymer constructs, Galban and Locke (1997) developed a distributed-parameter model based on a moving boundary analysis of cell growth coupled to a pseudosteady-state analysis of nutrient diffusion and utilization. They tested it against early global data from our laboratory (Freed et al., 1994b). The displacement of the cell/media interface as a function of time could be made to fit the data, but this required adjustment of the nutrient's cell-phase diffusivity and external mass-transfer coefficient for each new value of scaffold thickness. In a followup article, Galban and Locke (1999) refined their model by introducing terms for nutrient and product inhibition and cell death into their expression for cell growth kinetics. However, regressed parameters remained dependent upon scaffold thickness. Their pioneering efforts demonstrate both the potential and challenges of mathematical modeling of *in vitro* cartilage growth.

The recent development in our laboratory of a high-resolution image processing technique to monitor local concentrations of cell and GAG in histological tissue sections (Martin et al., 1999) allowed us to explore oxygen-dependent deposition of GAG (a marker of chondrogenesis) in growing tissue, and motivated development of a mathematical model of the associated diffusion/reaction processes. The conditions we chose to model were those identified as most favorable for engineering metabolically and mechanically functional cartilage: free suspension of constructs in dynamic laminar flow within rotating bioreactors. To minimize the number of adjustable parameters, cell density data was inserted directly into the algorithm. Our main objectives were to calculate GAG concentrations as a function of position within the tissue and cultivation time, and test them against data yielded by the high-resolution image processing.

Materials and Methods

Engineered cartilage constructs were obtained by culturing bovine chondrocytes on biodegradable polymer scaffolds in bioreactors at two different oxygen tensions in the culture medium. Constructs were sequentially removed at different stages of cultivation for assessment of spatial distributions of the cartilage marker glycosaminoglycan (GAG), via high-resolution image processing of histological sections. Additional

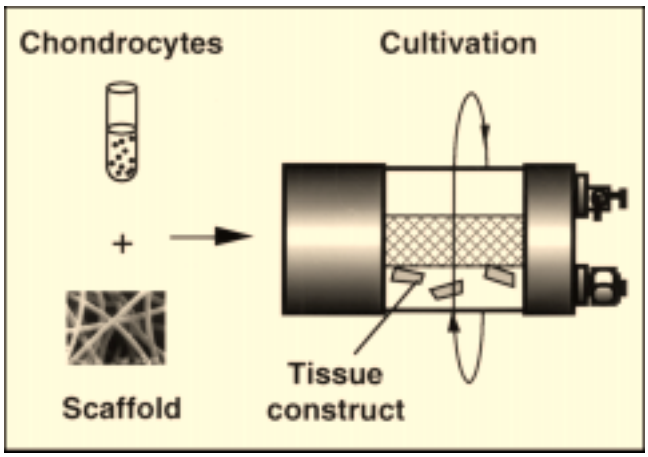

Figure 1. Model system.

Chondrocytes were isolated from bovine calf articular cartilage, seeded onto fibrous, biodegradable polyglycolic acid scaffolds (5-mm-dia.×2-mm-thick discs, 97% void volume) and cultured in rotating bioreactors. The vessel rotation rate is adjusted over the time of cultivation (such as 15 rpm at 3 days, 45 rpm at 6 weeks) to maintain each tissue construct settling at an approximately steady position within the vessel.

data was obtained, as indicated, from tissue samples grown in previous studies. GAG concentration profiles were used to validate the mathematical model, as described below.

Cell isolation

Engineered cartilage was obtained by culturing articular chondrocytes on biodegradable polymer scaffolds in bioreactors (Figure 1) as described previously (Freed and Vunjak-Novakovic, 1995; Freed et al., 1998). Full-thickness articular cartilage was harvested aseptically from femoropatellar grooves of 2–3-week-old bovine calves within 8 h of slaughter (Buschmann et al., 1992). A total of six knee joints was used. Chondrocytes were isolated with type II collagenase (Worthington, Freehold, NJ) and resuspended in a culture medium (Dulbecco's Modified Eagle Medium, DMEM, containing 4.5 g/L glucose and supplemented with 10% Fetal Bovine Serum, 10 mM N-2-HydroxyEthylPiperazine N′-2-EthaneSulfonicAcid, HEPES, 50 U/mL penicillin, 50 μg/mL streptomycin, 0.1 mM nonessential amino acids, 0.4 mM proline, 50 μg/mL ascorbic acid and 0.5 μg/mL fungizone) (Freed et al., 1993).

Scaffold seeding

Scaffolds were fibrous disks, 5 mm diameter × 2 mm, made from polyglycolic acid (PGA) by Albany International (Mansfield, MA) as highly porous mesh with 65 mg/cm^3 bulk density and 97% void volume (Freed et al., 1994c). A total of 24 scaffolds were seeded dynamically with freshly isolated chondrocytes as described previously (Vunjak-Novakovic et al., 1998). Briefly, scaffolds were prewetted in culture medium and threaded 5 mm apart onto 8-cm-long No. 22 gauge needles. Four needles with three scaffolds each were positioned symmetrically and affixed to a silicone stopper in the mouth

of a spinner flask (Bellco, Vineland, NJ). The flasks were filled with 120 cm^3 of culture medium and mixed at 50 rpm by a nonsuspended magnetic stirring bar (4 cm $\times$ 0.8 cm diameter), while housed in a humidified 37°C, 10% CO_2 incubator; gas exchange was promoted by surface aeration through loosened side-arm caps. After 18 h, medium was replaced with a suspension of freshly isolated chondrocytes (120 cm^3, 5×10^5 cells/cm^3, corresponding to 5×10^6 cells per scaffold).

Tissue culture

After three days of seeding in flasks, cell-polymer constructs were transferred into rotating bioreactors (two vessels, each containing $n=12$ constructs in 110 cm^3 medium) and cultured for up to six weeks. Rotating bioreactors (RCCV-110, Synthecon, Houston, TX) were each configured as the annular space between a 5.75-cm-ID outer polycarbonate cylinder and a 2-cm-OD hollow inner cylinder with a porous wall that was covered with a 175-μm-thick silicone membrane. Each vessel was rotated as a solid body in a horizontal plane around its central axis. The rotation rate was adjusted so as to suspend each tissue construct in rotational flow about a fixed position within the vessel as viewed by an external observer. In order to establish dynamic equilibrium of the operative forces (gravity, buoyancy, drag, and centrifugal force), while maintaining each tissue construct in a state of continuous free fall, the rotation rate was increased gradually from 15 to 45 rpm over the period of cultivation to accommodate the increase in construct weight (Freed and Vunjak-Novakovic, 1995). Sterile incubator gas (10% CO_2 in air) was blown through the inner cylinder at 700–1,200 cm^3/min; culture medium was supplied with oxygen and purged of excess CO_2 by diffusion through the silicone membrane. Medium was exchanged batchwise at a rate of 50% v/v, every other day. The resulting culture medium oxygen tension was approximately 80 mm Hg (77.6$\pm$3 mm Hg).

Additional data from our previous cartilage tissue engineering studies were used as follows. In one study carried out for a period of 5 weeks (Obradovic et al., 1999), gas exchange in rotating bioreactors was either continuous as described above, or eliminated by replacing the hollow inner cylinder with a solid one. The resulting culture medium oxygen tensions, p_{O_2} values of 86.5 $\pm$ 7.3 and 42.7 $\pm$ 4.5 mm Hg, respectively, reflected O_2 supply primarily from the hollow cylinder or by diffusion through the vessel walls. The profiles of GAG concentration C_G in construct sections after five-week cultivation at low medium p_{O_2}, which are reported here for the first time, were used to test the model under hypoxic conditions. In addition to samples from the present study, constructs cultured for up to 6 weeks at a p_{O_2} of approximately 80 mm Hg (Freed et al., 1998) were analyzed to determine the maximum C_G value. Additional data obtained in the latter study were used in the present study to determine the cultivation-time dependence of the parameter k in the kinetic expression for GAG synthesis.

Analytical assays

Constructs were sampled at timed intervals for biochemical (n = 3–4) and histological (n = 2) analyses. Samples for biochemical analysis were frozen, lyophilized, and digested for 15 h at 56° C with 1 mg/cm^3 protease-K in buffer solution (50 mM Tris, 1 mM EDTA, 1 mM iodoacetamide, 10 μg/cm^3 pepstatin A), using 1 cm^3 of this solution per 4–10 mg dry weight (Hollander et al., 1994). The chondrocyte number was obtained from the amount of DNA measured spectrofluorometrically (Aminco, Urbana, IL) using Hoechst 33258 dye (Kim et al., 1988) and conversion factors of 7.7 pg DNA (Kim et al., 1988), as well as 10^{-10} g dry weight (Freed et al., 1994c) per chondrocyte. The total amount of glycosaminoglycan (GAG) was determined spectrophotometrically after reaction with dimethylmethylene blue dye, using bovine chondroitin sulfate standard (Farndale et al., 1986).

Samples for histological analysis were fixed in 10% neutral buffered formalin, embedded in paraffin and cross-sectioned (5-μm thick). The sections were stained with hematoxylin and eosin for cells, and safranin-O/fast green for GAG.

GAG distributions in constructs and construct dimensions were assessed from histological sections stained with safranin-O, via high-resolution image analysis as described previously (Martin et al., 1999). In brief, images were obtained using a solid-state 3 CCD camera (Hitachi HV-C20) mounted on a Nikon Diaphot inverted microscope. Red, green and blue (RGB) image planes were digitized on a scale of 256 values using an LG-3 frame grabber (Scion Corporation, Frederick, MD) and analyzed using IPLab Spectrum software (Sigma Analytics Corporation, Vienna, VA). Red color intensity of a histological section (average value for whole section) was correlated to construct GAG wet weight fraction. Experimental GAG distributions were determined by automated measurement of average red intensity in 41.7-μm-thick concentric annular regions of whole tissue sample cross-sections. For each region, the wet weight fraction of GAG was determined using the previously established correlation between the red intensity and biochemically measured GAG fraction (r^2 = 0.952, p < 0.0001, for GAG fractions ranging from 0.5 to 7.0% ww; Martin et al., 1999). Thickness and diameter of each construct section were determined by averaging 5 measurements.

Cell distributions within constructs were determined from H&E-stained histological sections as previously described (Vunjak-Novakovic et al., 1998). In brief, black and white images (n = 15–20 per sample) were acquired at successive tissue depths as described above, digitized by a CG-7 frame grabber (Scion Corp., Frederick, MD) and analyzed using Scion-Image software (Scion Corp., Frederick, MD). The total area of each image, 0.245 mm^2, was divided automatically into 24 windows, 20.4 $\times$ 500 μm each. Cell number was determined by counting of all objects darker than background, except for undegraded polymer fibers, which were manually excluded from each image. Spatial and temporal changes in cell density were determined from average numbers of cells per unit image area.

Spatial and Temporal Patterns of Matrix Deposition

Progressive structural changes were consistent with previously reported spatial and temporal patterns of *in vitro* chondrogenesis (Freed et al., 1998). Freshly seeded constructs consisted of uniformly distributed cells attached to polymer fibers. Cells at the construct periphery proliferated more

rapidly, presumably due to direct contact with medium. Concomitant deposition of GAG and collagen also started at the construct periphery, and progressed apositionally, both inward and outward. After 10–12 days of cultivation, each construct consisted of a layer of compact peripheral cartilaginous matrix surrounding a central region which still contained large empty pores (Figure 2). Construct size and shape remained approximately constant over the first 12 days of cultivation, reflecting comparable rates of polymer degradation and matrix synthesis. Further deposition of extracellular matrix, ECM, depended strongly on oxygen availability.

Cell-polymer constructs cultivated in this study at a p_{O_2} of 80 mm Hg gained significantly in size and weight. The presence of undegraded fibers only in the inner zones of constructs, and not in their external regions, suggested growth by formation of new tissue at the periphery. Growth in axial and radial directions maintained the initial discoidal construct shape. Constructs cultivated for 6 weeks appeared uniformly cartilaginous and were twice as heavy as those cultured for 10 days (Figure 2). In our earlier experiments carried out at high and low p_{O_2} (86.5 $\pm$ 7.3 and 42.7 $\pm$ 4.5 mm Hg) under otherwise identical conditions (Obradovic et al., 1999), oxygen availability markedly affected tissue development. Although the respective construct cellularities after 5 weeks of culture at high and low oxygen tension were essentially the same (0.97 $\pm$ 0.09 and 0.99 $\pm$ 0.15% ww)., their wet weights were 139 $\pm$ 12 and 101 $\pm$ 8 mg/construct, respectively, and their GAG contents were 4.18 $\pm$ 0.22 and 3.07 $\pm$ 0.28% ww, respectively.

Similar O_2 sensitivity had been observed in perfused bioreactor cultures of cartilage explants, where a gradual decrease in p_{O_2} from $\sim$80 to $\sim$40 mm Hg resulted in a shift from aerobic to anaerobic cell metabolism, and eventually the suppression of tissue growth (Obradovic et al., 1997). Likewise, GAG synthesis rates in cartilage explants were twice as high at p_{O_2} = 78–180 mm Hg as at 45 mm Hg (Ysart and Mason, 1994). However, not all published data were consistent. GAG synthesis rates in monolayers of bovine and rabbit chondrocytes were markedly higher at p_{O_2} = 140–160 than at 20–50 mm Hg (Clark et al., 1991; Marcus, 1973). Notably, however, a low p_{O_2} of 8 mm Hg stimulated GAG synthesis in a short-term study of bovine chondrocyte monolayers (Neitzel et al., 1998). *In vivo*, immature articular cartilage, which is still vascularized and thus efficiently supplied with oxygen, exhibits high biosynthetic activity. In contrast, skeletally mature cartilage, where oxygen must diffuse from the articular surface,

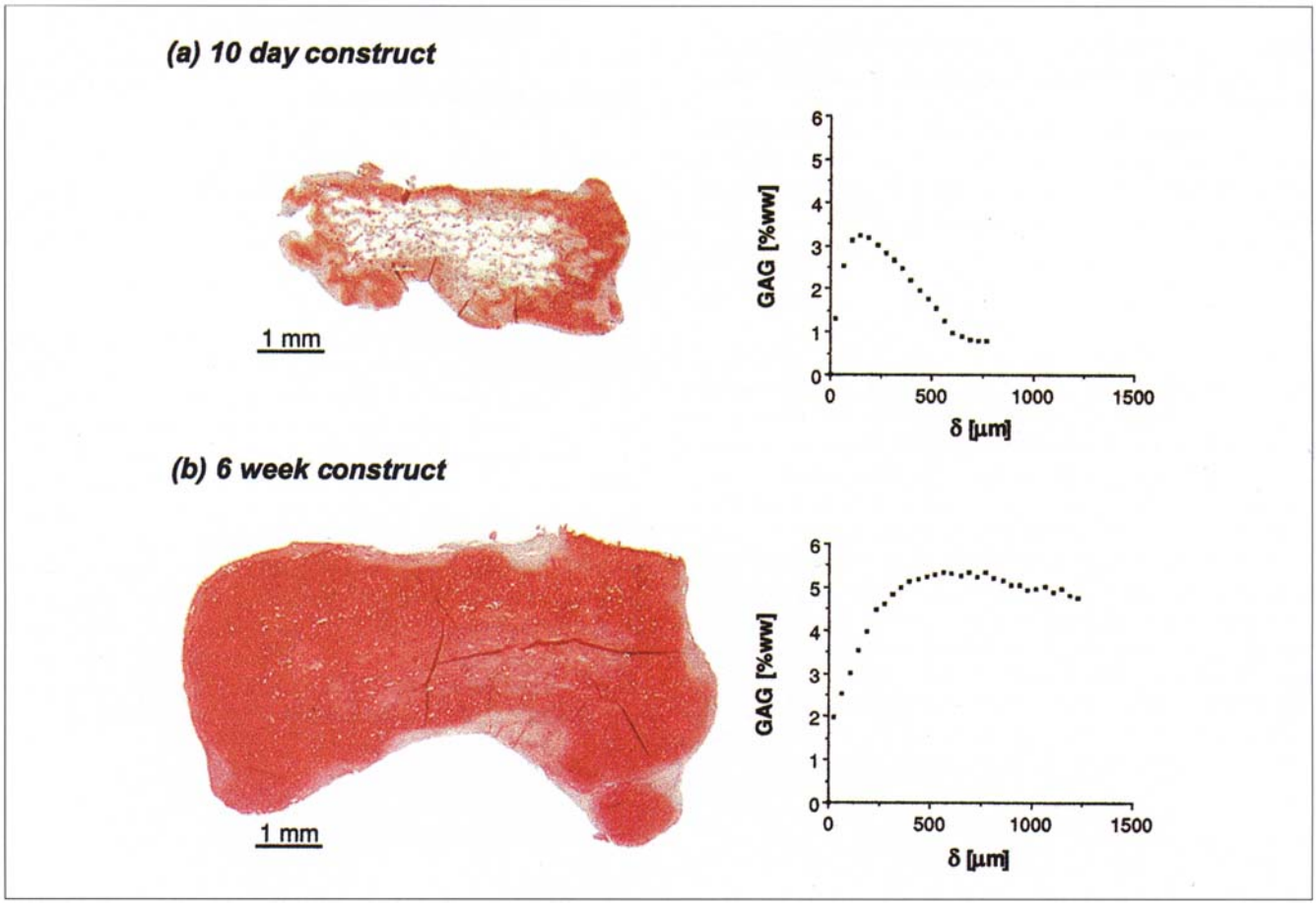

Figure 2. Progression of cartilaginous matrix deposition.

Representative histological cross-sections of cartilage constructs cultured for (a) 10 days and (b) six weeks at culture medium oxygen tension of p_{O_2} = 80 mm Hg. The corresponding GAG distribution profiles (C_G, wet weight fraction of GAG within a 41.7 μm thick layer of tissue at a distance δ from the construct surface) were determined by image processing of histological sections. Stain: safranin-O/fast green.

exhibits low biosynthetic activity and practically no capacity for tissue growth or repair. Taken together, the available data suggest that immature cartilage, whether native or engineered, has significant biosynthetic capacity for GAG deposition, and that the rate of GAG deposition is positively correlated to the local oxygen concentration.

Model Equations

A mathematical model was developed in order to rationalize the profiles of GAG concentration measured as a function of cultivation time in disc-shaped cartilage constructs. The central hypothesis, consistent with the weight of the above-cited evidence, was that the rate of GAG deposition depends on local O_2 concentration.

Temporal changes in local oxygen concentrations C_{O_2} within tissue constructs were assumed to be governed by diffusional transport and cellular consumption at the rate q_{O_2}, that is,

$$\frac{\partial C_{O_2}}{\partial t} = D_{O_2}\left(\frac{\partial^2 C_{O_2}}{\partial r^2} + \frac{1}{r}\frac{\partial^2 C_{O_2}}{\partial r^2} + \frac{\partial^2 C_{O_2}}{\partial z^2} + \frac{1}{r^2}\frac{\partial^2 C_{O_2}}{\partial \theta^2}\right) - q_{O_2} \quad (1)$$

where D_{O_2} is the effective oxygen diffusion coefficient, r, z and θ are cylindrical coordinates (Figure 3a), and t is time of cultivation.

Oxygen consumption, which includes O_2 utilization for both energy metabolism and matrix biosynthesis, was assumed to follow Michaelis-Menten kinetics as reported previously for isolated chondrocytes (Haselgrove et al., 1993)

$$q_{O_2} = \rho \cdot \frac{Q_m C_{O_2}}{C_m + C_{O_2}} \quad (2)$$

where ρ is cell density, Q_m is the maximal O_2 consumption rate, and C_m is the C_{O_2} at half-maximal O_2 consumption. It is implicitly assumed that the magnitude of cellular O_2 consumption is insensitive to the rate of GAG synthesis.

It was also assumed that O_2 promotes deposition of GAG, which is synthesized and assembled intracellularly into proteoglycan monomers, then secreted into the extracellular matrix. Although most proteoglycan monomers aggregate, all proteoglycan species were treated as mobile, since they are reportedly released into the media of cartilage explant cultures (Bolis et al., 1989; Campbell et al., 1989). For simplicity, they were assigned a single effective diffusion coefficient D_G.

Thus, profiles of GAG concentration (C_G) were assumed to be mediated by diffusion and reaction according to

$$\frac{\partial C_G}{\partial t} = D_G\left(\frac{\partial^2 C_G}{\partial r^2} + \frac{1}{r}\frac{\partial^2 C_G}{\partial r^2} + \frac{\partial^2 C_G}{\partial z^2} + \frac{1}{r^2}\frac{\partial^2 C_G}{\partial \theta^2}\right) - q_G \quad (3)$$

The effective local GAG synthesis rate q_G reflects simultaneous GAG production, degradation, and incorporation into the matrix. In healthy cartilage *in vivo*, cells maintain steady-state metabolism of proteoglycans by balancing proteoglycan synthesis and catabolism (Hascall et al., 1999). In engineered constructs, GAG deposition begins at the construct periphery, where a high cell density promotes more rapid GAG synthesis than catabolism. Over the time of cultivation, a limiting steady-state concentration Cl is approached at which there is a balance of production, degradation, and incorporation. Accordingly, local GAG kinetics were formulated as product-inhibited, with Cl the maximum GAG concentration. The dependence upon C_{O_2} was modeled as first-order based on the relative success of models with Michaelis-Menten and zero-, first-, and second-order dependence on C_{O2}. Thus, GAG synthesis kinetics were formulated as

$$q_G = \rho \cdot k \cdot \left(1 - \frac{C_G}{Cl}\right) C_{O_2} \quad (4)$$

where k is the rate constant.

Finally, construct symmetry make composition independent of θ. The governing equations, coupled by dependence

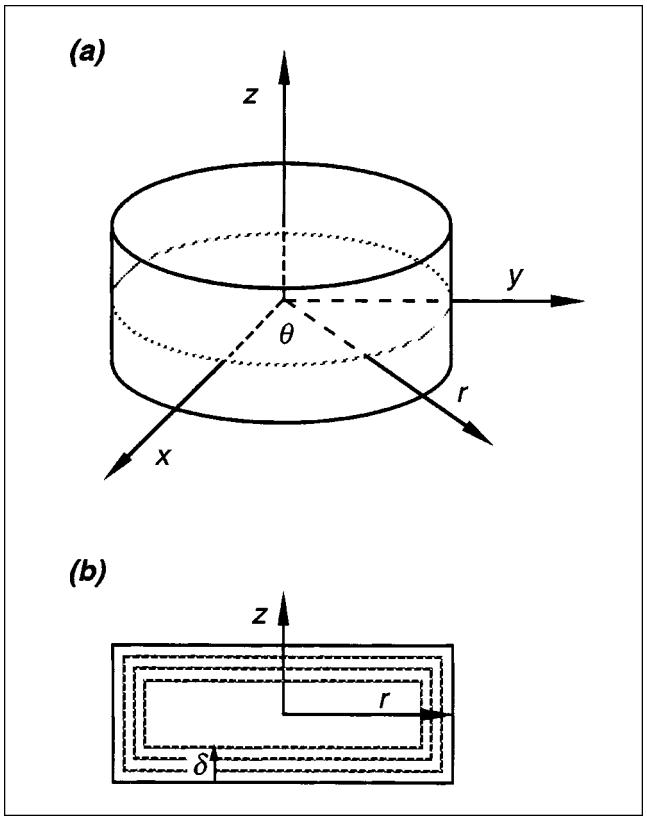

Figure 3. Construct geometry.

(a) Concentration profiles of oxygen and GAG within the tissue were modeled using cylindrical coordinates (z, r, $\theta = 0$ at the construct center); (b) concentration profiles of GAG were experimentally determined within 41.7 μm thick annular rings in tissue cross-sections as a function of the distance δ from the construct surface.

of GAG synthesis on C_{O_2}, thereby reduce to

$$\frac{\partial C_{O_2}}{\partial t} = D_{O_2}\left(\frac{\partial^2 C_{O_2}}{\partial r^2} + \frac{1}{r}\frac{\partial C_{O_2}}{\partial r} + \frac{\partial^2 C_{O_2}}{\partial z^2}\right) - \rho \cdot \frac{Q_m C_{O_2}}{C_m + C_{O_2}} \tag{5}$$

$$\frac{\partial C_G}{\partial t} = D_G\left(\frac{\partial^2 C_G}{\partial r^2} + \frac{1}{r}\frac{\partial C_G}{\partial r} + \frac{\partial^2 C_G}{\partial z^2}\right) + \rho \cdot k \cdot \left(1 - \frac{C_G}{Cl}\right) C_{O_2} \tag{6}$$

Initial and boundary conditions

Cell-polymer constructs were initially free of GAG and equilibrated with medium at p_{O_2}, that is,

$$\left.\begin{aligned} C_G &= 0 \\ C_{O_2} &= C^0_{O_2} \end{aligned}\right\} \quad t = 0; \quad 0 \le r \le d/2; \quad 0 \le z \le h/2 \tag{7}$$

where d is construct diameter, h is construct thickness and $C^0_{O_2}$ is the concentration of physically dissolved O_2 in equilibrium with p_{O_2}.

Periodic partial medium exchange (50% v/v, every other day) and continuous gas exchange ensured quasi-steady external conditions after an initial cultivation period (Obradovic et al., 1999). Furthermore, settling of tissue constructs promoted mixing of vessel contents (equivalent to 1.1 mixed tanks in series; Freed and Vunjak-Novakovic, 2000b). External mass-transfer resistance was therefore neglected. Accordingly, solute concentrations at construct surfaces were

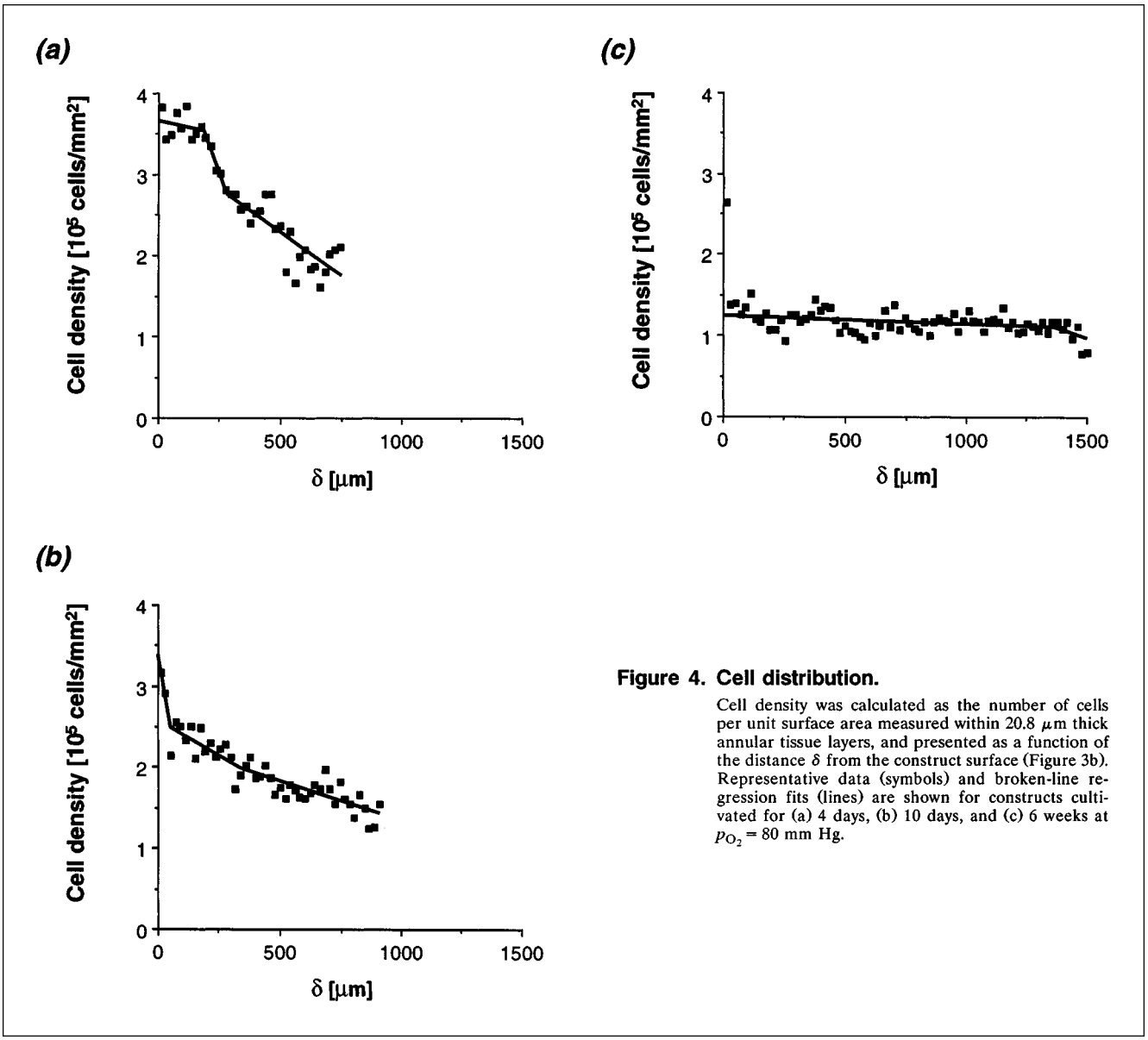

Figure 4. Cell distribution.

Cell density was calculated as the number of cells per unit surface area measured within 20.8 μm thick annular tissue layers, and presented as a function of the distance δ from the construct surface (Figure 3b). Representative data (symbols) and broken-line regression fits (lines) are shown for constructs cultivated for (a) 4 days, (b) 10 days, and (c) 6 weeks at p_{O_2} = 80 mm Hg.

set equal to steady-state values measured in bulk medium, as follows

$$\left.\begin{array}{c} C_G = 0 \\ C_{O_2} = C^0_{O_2} \end{array}\right\} \quad t > 0; \quad \begin{array}{l} r = d/2; \quad 0 \le z \le h/2 \\ z = h/2; \quad 0 \le r \le d/2 \end{array} \tag{8}$$

Finally, symmetry conditions were enforced along construct central axes, that is

$$\left.\begin{array}{c} \dfrac{\partial C_G}{\partial r} = 0 \\ \dfrac{\partial C_{O_2}}{\partial r} = 0 \end{array}\right\} \quad t > 0; \quad r = 0; \quad 0 \le z \le h/2 \tag{9}$$

$$\left.\begin{array}{c} \dfrac{\partial C_{O_2}}{\partial z} = 0 \\ \dfrac{\partial C_{O_2}}{\partial z} = 0 \end{array}\right\} \quad t > 0; \quad z = 0; \quad 0 \le r \le d/2 \tag{10}$$

Construct dimensions d and h were forced to vary with time in accordance with experimental observations. For the first 12 days, they were assigned fixed values consistent with approximation of the geometry of a freshly seeded polymer scaffold by a cylinder (5.5 mm diameter $\times$ 1.9 mm). Between 12 days and 6 weeks, d and h increased at constant rates of 70 and 50 μm/day, respectively, at $p_{O_2} = 80$ mm Hg, and negligibly at $p_{O_2} = 40$ mm Hg.

Numerical solution

Equations 5 and 6 were solved using the alternating-direction implicit finite difference method (von Rosenberg, 1969) which facilitates linearization over small time intervals. Equation 5 was may be solved independently, because it does not contain C_G. The resulting C_{O_2} profiles were inserted in Eq. 6, which was then solved to derive C_G profiles.

To model construct growth, spatial mesh points were added at appropriate times between points at surfaces and immediately adjoining locations. Values of C_G and C_{O_2} at newly added points were initially set midway between those at the latter two sites.

Calculated GAG concentrations were compared with experimental values determined by image processing of 41.7-μm-thick construct sections. For this purpose, calculated GAG concentrations were averaged over the appropriate regions.

Model Parameters

The mathematical model requires values for the following parameters: cell density ρ, diffusion coefficients D_{O_2} and D_G, limiting GAG concentration Cl, Michaelis-Menten constant C_m, maximal O_2 consumption rate Q_m, and GAG synthesis rate constant k.

Cell density distributions

Cell density distributions were determined in 4-day, 10-day and 6-week constructs by image analysis of histological cross-sections; the results are shown in Figure 4 (data points). Cell density was measured in each 20.8 μm annular layer within a construct and presented as a function of the distance δ (measured from the center of the layer) to the tissue surface ($\delta = 0$). For each time point, cell density was fit by broken-line regression as a function of δ (Figure 4, lines). Then it was fit as a function of time

$$\rho(\delta, t) = m_1 e^{-m_2 t} + m_3 \tag{11}$$

where sets (m_1, m_2, m_3) were determined at the discreet δ values.

Oxygen diffusion coefficient

D_{O_2} in constructs was set at 1.5×10^{-5} cm^2/s, or approximately 50% of D_{O_2} in water, in light of values reported for intact cartilage that range from 30 to 80% of D_{O_2} in water (Maroudas, 1979; Haselgrove et al., 1993).

GAG diffusion coefficient

D_G was estimated by inserting values for the GAG concentration gradient within the construct and the rate of GAG release into medium, measured under conditions of constant construct dimensions and essentially uniform medium composition, into the equation

$$V_{med} \frac{dC_{Gmed}}{dt} = D_G S \left.\frac{\partial C_G}{\partial \delta}\right|_{\delta = 0} \tag{12}$$

where the medium volume V_{med} was 120 cm^3 and the total surface area S of all constructs ($n = 11$) in the reactor vessel was 0.88 cm^2. The possibility of internal convection associated with GAG release was rejected in light of observations of (1) continuous surface layers of compact cartilaginous tissue within 7–10 days of culture, and (2) decreases in construct permeability between days 3 and 7 (Freed et al., 1994b).

A GAG release rate dC_{Gmed}/dt of 1.90×10^{-5} g/dL·h was determined by a least-squares straight-line fit of the cumulative amount released vs. time ($r^2 = 0.99$). A GAG concentration gradient $(\partial C_G/\partial \delta)_O$ $\delta = 0$ of 9.7 $\times 10^{-3}$ g/cm^2/cm was similarly derived ($r^2 = 0.87$) from the GAG concentration profile measured by image analysis of histological cross-sections. The apparent D_G value of 7×10^{-11} cm^2/s falls in the range reported for proteoglycan monomers and aggregates in concentrated solutions (Comper and Williams, 1987). Because the apparent D_G is this low, the GAG diffusion time is far greater than the maximum cultivation time. It follows that except for the release of GAG into the culture medium, its diffusive transport is negligible, that is, in Eq. 6

$$\left|\frac{\partial C_G}{\partial t}\right| \gg D_G \left|\frac{\partial^2 C_G}{\partial x^2}\right|$$

Maximal GAG concentration in constructs Cl

After 6 weeks of cultivation in rotating bioreactors, Cl was determined by sectional image analyses to range from 5.0 to 5.7% ww. The value inserted in model calculations 5.5% ww

is consistent with the 5–6% ww range measured in earlier related studies (Obradovic et al., 1999; Martin et al., 1999) and the value of $6.1 \pm 0.3\%$ ww measured in native cartilage explants (Obradovic et al., 1997; Vunjak-Novakovic et al., 1999).

Michaelis-Menten constant

C_m was set at the value of 0.006 mM reported for chick growth plate chondrocytes in the prehypertrophic zone (Haselgrove et al., 1993).

Maximal cellular O_2 consumption rate in constructs

Q_m was estimated on the basis of the rate of decrease in culture medium C_{O_2} following gas exchange, and the assumption that constructs consumed oxygen uniformly at this zero-order rate (an assumption borne out by the calculated tissue oxygen profiles described below). As eleven cell-polymer constructs were grown in 110 cm^3 of medium for 5 weeks, C_{O_2} was measured in medium samples withdrawn periodically between medium exchanges. The estimated O_2 consumption rate of 1.86×10^{-18} mol/cell·s exceeds somewhat the $0.6–1.6 \times 10^{-18}$ mol/cell·s range reported for chondrocytes in bovine articular cartilage (Marcus, 1973).

Rate constant of GAG synthesis

k was estimated using Eq. 4 in conjunction with previously measured biochemical rates of GAG synthesis in engineered constructs (Freed et al., 1998) as follows. Equation 4 relates GAG synthesis rate to the oxygen and GAG concentrations and cell density. All other factors that may affect GAG synthesis to varying degrees over time (such as cell metabolism and growth factors) are presumed to be accounted for by the kinetic parameter k. Apparent k values were derived indirectly from the sulfate incorporation rates q_S measured in an earlier study at timed intervals over six weeks of construct cultivation in rotating vessels at $p_{O_2} \sim 80$ mm Hg (Freed et al., 1998). Values of q_s (which are proportional to q_G) (Kuettner et al., 1982) and biochemically measured construct GAG concentrations $C_{G,\text{ave}}$ were inserted into Eq. 4 in order to estimate values for the kinetic parameter of sulfate incorporation k' defined by

$$q_S = k'\left(1 - \frac{C_{G,\text{ave}}}{Cl}\right) \tag{13}$$

Note also that constant average values of C_{O_2} and ρ were presumed to be reflected in k'.

Values of k' were essentially constant ($\equiv k'_0$) over the first 12 days of cultivation, then increased linearly with time according to

$$k' = k'_0\left[1 + A(t - t_0)\right] \qquad t \geq t_0 = 12 \text{ days} \tag{14}$$

The parameter A at $p_{O_2} = 80$ mm Hg was estimated at 0.11 day^{-1} via least-squares fit to the entire set of k' vs. t data ($r^2 = 0.96$), and used to calculate the GAG synthesis kinetic parameter k as a function of time, that is, by applying Eq. 14 without primes. The estimated value of A at $p_{O_2} = 40$ mm Hg was effectively 0; thus, k_0 corresponds to the observed constant rate of GAG deposition at these conditions of construct cultivation.

The experimentally determined model parameters are summarized in Table 1.

Model Calculations

Cultivation at O_2 tension of 80 mm Hg

The mathematical model was used to calculate first oxygen (Eq. 5) and then GAG (Eq. 6) concentration profiles. For

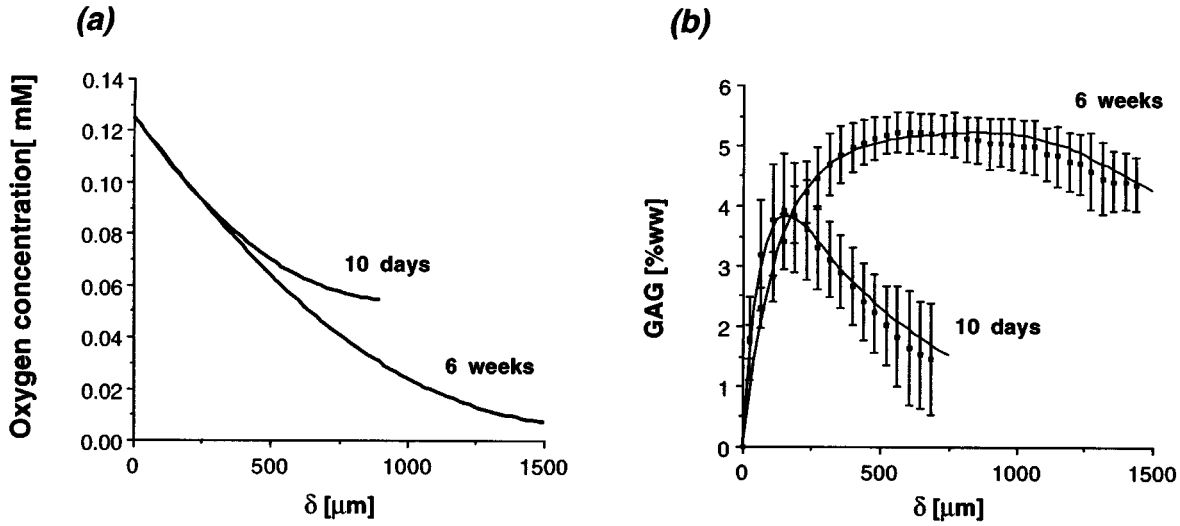

Figure 5. Model predictions of oxygen and GAG distribution in constructs cultivated for ten days and six weeks at $p_{O_2} = 80$ mm Hg.

(a) Calculated oxygen concentration profiles; (b) GAG concentration profiles measured by image processing of construct sections (symbols, average $\pm$SD, $n = 2–4$), and calculated using model equations (lines).

Table 1. Model Parameters

Parameter	Value	Reference
D_{O_2} (cm^2/s)	1.5×10^{-5}	Haselgrove et al. (1993)
D_G (cm^2/s)	7×10^{-11}	This work
Cl (%ww)	5.5	This work
Q_m (mol/cell·s)	1.86×10^{-18}	This work
C_m (mM)	0.006	Haselgrove et al. (1993)
A (d^{-1})	0.11	This work

constructs grown for up to 6 weeks at $p_{O_2} = 80$ mm Hg, the results are depicted in Figures 5a and b. Calculated C_{O_2} values decreased with time as shown in Figure 5a.

Adjustable parameter k_0 was estimated at 2.3% ww GAG day^{-1} $mM_{O_2}^{-1}/[10^5$ cell/$mm^3]$ by a least-squares fit of model output to the C_G profile measured in 10-day constructs (Figure 5b). All remaining model calculations were based on the fixed parameter set listed in Table 1. As shown in Figure 5b, the calculated C_G profile at six weeks (by which time k had increased approximately 4-fold) is in excellent agreement with the experimental data (mean SD = ±0.2% ww GAG).

Cultivation at O_2 tension of 40 mm Hg

The model was tested further against C_G profiles measured in the constructs grown earlier for 5 weeks at the lower

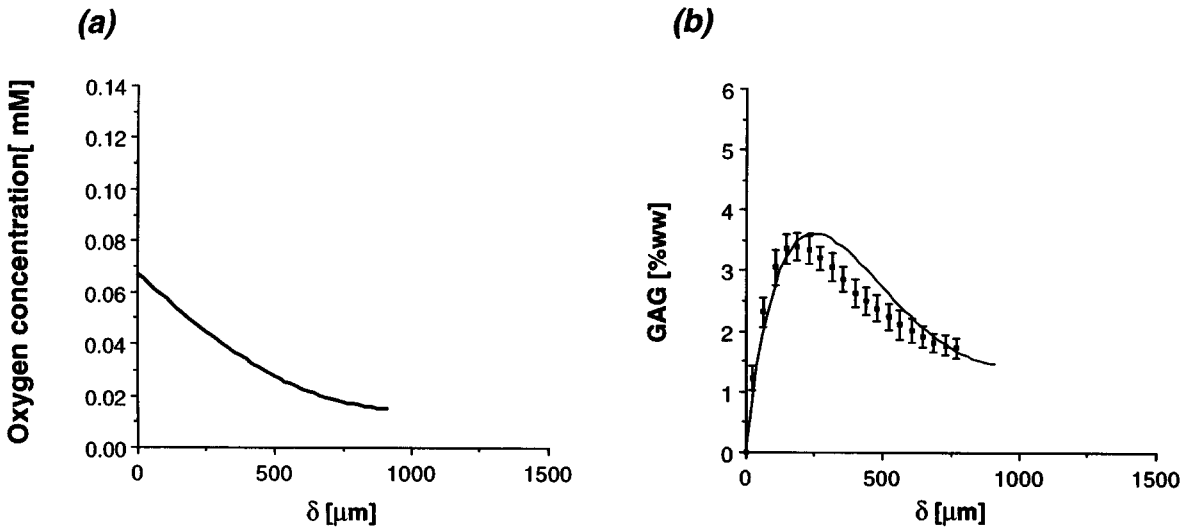

Figure 6. Model predictions of oxygen and GAG distribution in constructs cultivated for five weeks at $p_{O_2} = 40$ mm Hg.

(a) Calculated oxygen concentration profiles; (b) GAG concentration profiles measured by image processing of construct sections (symbols, average ±SD, $n = 2$–4), and calculated using model equations (lines).

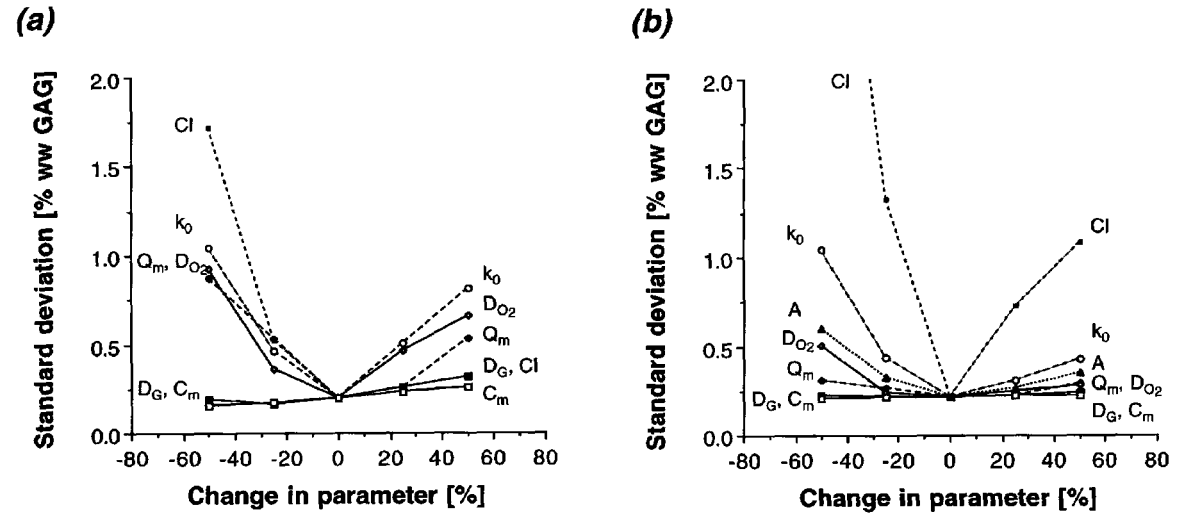

Figure 7. Sensitivity analysis.

Standard deviations between model predictions and experimental data as functions of model parameters for (a) ten-day and (b) six-week constructs. For each parameter, 0 refers to the base line value used to solve the model equations.

p_{O_2} of 40 mm Hg. The calculated C_{O_2} profile is shown in Figure 6a. The corresponding C_G profile, shown in Figure 6b, is in good qualitative and fair quantitative agreement with the data (mean SD = ±0.3% ww GAG).

Reproducibility and sensitivity analysis

Reproducibility of experimentally determined C_G profiles was assessed by comparing 14 histological sections of constructs cultivated for either 10 days or six weeks, in three independent experiments carried out under identical conditions (Freed et al., 1998; Obradovic et al., 1999; this study). A comparison was made of C_G values measured after the same cultivation times, in annular rings the same distance from the construct surface. The overall standard deviation in serial sections of 14 tissue samples was ±13%.

The sensitivities of model C_G profiles to changes in model parameters (±50% of base line values) were evaluated at 10 days and 6 weeks in terms of both (a) the standard deviation (SD) between calculated values and experimental data (Figure 7), and (b) the appearance of calculated C_G profiles (Figure 8). With the single exception of *Cl*, predictions were more sensitive to parameter changes at the earlier stage of cultivation. Furthermore, calculated results were, quantitatively, particularly sensitive to changes in *Cl*, k_0, D_{O_2} and Q_m, and insensitive to changes in C_m and D_G, as anticipated above; qualitatively, model predictions were most sensitive to changes in *Cl* and D_{O_2}. By definition, *Cl* determined the maximum obtainable C_G (Figures 8a and 8b); D_{O_2} influenced C_G profiles by way of C_{O_2} (Figures 8c and 8d).

Discussion

To recapitulate, it was anticipated that a simple first-approach model would be consistent with the observed progression of chondrogenesis if it faithfully accounted for time-dependent local rates of synthesis, and consumption and diffusion of oxygen and GAG. Production of GAG was taken as a marker of overall chondrogenesis in light of prior association of GAG deposition with that of collagen type II, the other

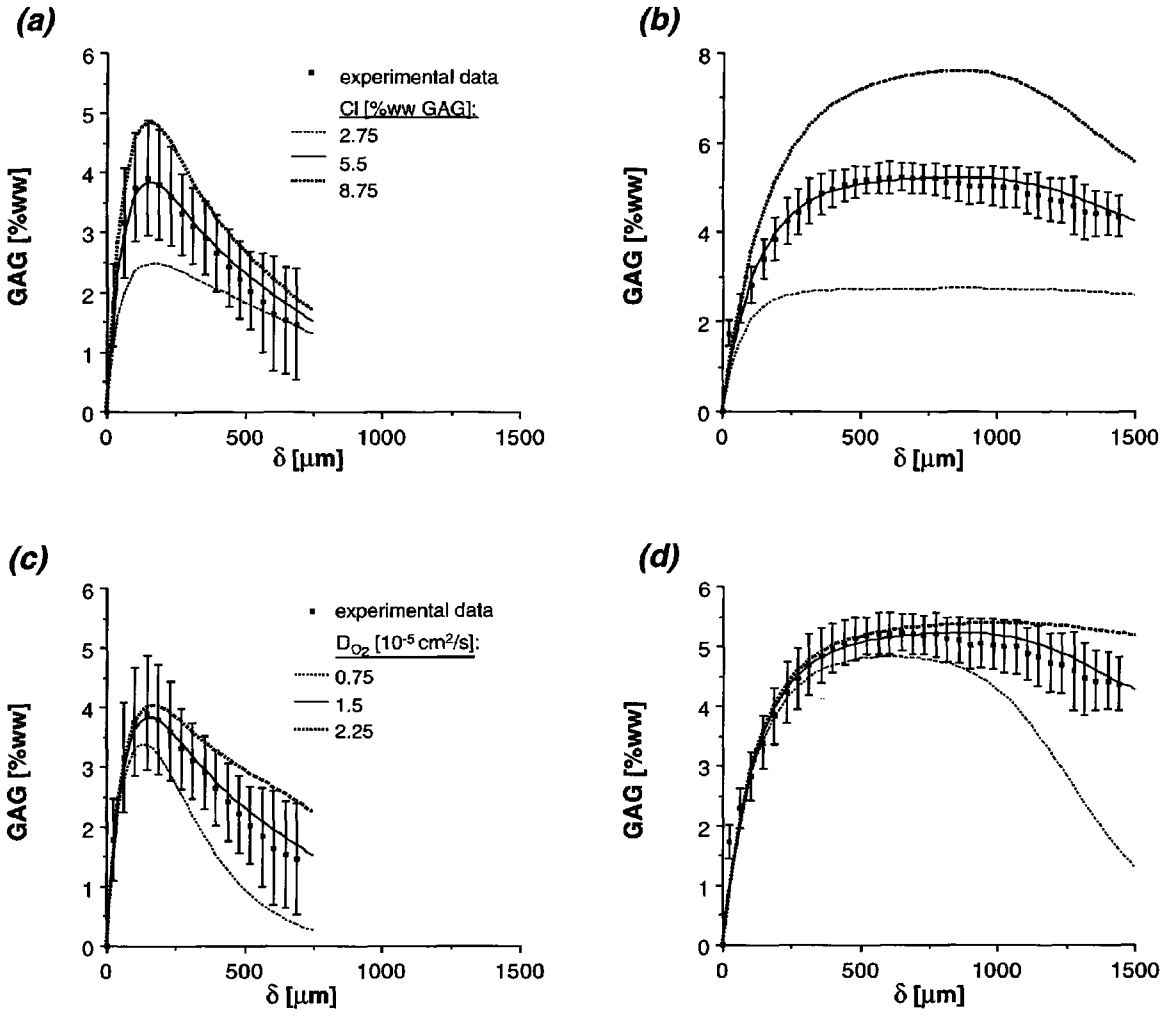

Figure 8. Sensitivity analysis.

Examples of qualitative changes in the appearance of predicted concentration profiles. Experimental GAG concentration profiles (symbols, average ± SD, $n = 2$–4) and model predictions (lines) obtained for ten-day (a, c) and six week constructs (b, d) for different values of *Cl* (a, b) and D_{O_2} (c, d).

major component of cartilage tissue matrix (Freed et al., 1998). The model was based on reasonable assumptions and on parameters that had been determined independently (in the sense that they evolved either from entirely different experiments, or from isolated data sets) with the exception of kinetic parameter k_0, which was obtained from a best fit to the entire set of C_G data obtained after 10 days of cultivation at $p_{O_2} = 80$ mm Hg. The model was tested without further parameter adjustment by comparison of calculated C_G profiles with those measured after cultivation at two different p_{O_2} values for different periods of time (Figures 5 and 6).

Model predictions were most sensitive to factors controlling GAG synthesis, either directly (k_0, A, Cl) or via local values of C_{O_2} (D_{O_2}, Q_m). Deviation of Cl from its experimentally determined base line value markedly affected C_G profiles, both quantitatively (Figure 7) and qualitatively (Figures 8a and 8b). Deviation of k_0 or A from base line values increased the SD of model predictions (Figure 7) without changing general trends, suggesting that factors other than O_2 and GAG (such as cell-derived signals) may significantly affect C_G profiles.

The effects of changes in D_{O_2} and Q_m on model accuracy were substantial, particularly at early stages of cultivation (Figure 7a), consistent with the hypothesized direct effects of oxygen on GAG synthesis. In contrast, changing D_G had little effect other than in the superficial tissue layer in contact with culture medium (Figure 7), consistent with a small role of GAG diffusion, as was anticipated above in light of the very small value of D_G. Similarly, model results were insensitive to changes in C_m (Figure 7), since, as is apparent in Figures 5a and 6a, $C_{O_2} \gg C_m$ essentially throughout the tissue.

The proposed model supports a first-order dependence of GAG synthesis on C_{O_2}, However, the exact mechanisms that regulate GAG synthesis, catabolism, and deposition remain largely unknown. It has been suggested that oxygen's effect is mediated by aerobic cell metabolism that provides energy to enhance GAG synthesis (Scott, 1992; Ysart and Mason, 1994), and that oxygen might be involved directly in the sulfation step of GAG synthesis (Scott, 1992). Lack of oxygen reportedly suppresses collagen synthesis in periosteal tissue explants and engineered cartilage (O'Driscoll et al., 1997; Obradovic et al., 1999), and causes markedly reduced construct wet weight after five weeks of cultivation without affecting cellularity (Obradovic et al., 1999). Formation of the collagen network, the structural template for immobilization of proteoglycan molecules, is another potential regulator of proteoglycan metabolism (Hascall et al., 1999).

The second hypothesis supported by the model is product inhibition of GAG synthesis, that is, a feedback mechanism whereby cells control their immediate environment. This may explain why cartilage engineered in various *in vitro* studies under favorable conditions (with respect to p_{O_2}, pH, and physicochemical regulatory signals) attained GAG levels that differed by less than 13% and approached those measured in natural cartilage explants (Obradovic et al., 1999; Vunjak-Novakovic et al., 1999). Again, the detailed regulatory mechanism remains to be elucidated.

The available evidence suggests that GAG metabolism is mediated by several extracellular factors, some of which (such as serum and growth factors) enhance GAG synthesis while others (such as interleukin-1, lypopolysaccharide, and retinoic acid) enhance GAG catabolism (Hascall et al., 1999). Notably, the kinetic parameter k of GAG synthesis, presumed here to encompass the above and other factors, remains nearly constant for the first 12 days of culture, during which time constructs do not enlarge but nonetheless undergo chondrogenesis at a rate that depends on oxygen availability. Beyond 12 days, k increases steadily at sufficiently high p_{O_2}, as reflected in the formation of continuously cartilaginous tissue (Figure 5b). However, at low p_{O_2}, k remains constant at k_0 and GAG production remains low (Figure 6b).

A possible explanation is that, at a certain stage of tissue development, cell-secreted growth factors, not initially present in the medium, trigger enhanced GAG synthesis, and that the appearance and/or biochemical effects of these factors are oxygen-sensitive. Alternatively, the initial rapid synthesis of a protective cartilaginous layer at the construct periphery might provide core cells with a more ''physiological'' environment, while promoting accumulation of cell-secreted growth factors. The greater sensitivity of 10-day as compared to six-week constructs suggests a pronounced early need for oxygen.

The main objectives in modeling were: (1) to rationalize our experimental data on local accumulation of GAG within engineered cartilage, obtained via a novel image processing technique with ~ 40-μm resolution, and (2) to relate this data to earlier observations of the dependence of global (2–5 mm scale) tissue properties on cultivation conditions (the domain of the focus in each case being limited by available analytical tools). The model presented here grossly approximates the processes that control tissue development. However, the consistency of model predictions with experimental data suggests that rate-controlling steps have at least been taken into account, and that simplifications do not distort actual behavior. For the model to serve as a predictive tool, it must incorporate other aspects of tissue development (such as cell growth and collagen deposition). Furthermore, as information is accumulated about biochemical pathways involved in regeneration of other tissue components (such as type II collagen), the model may be refined to facilitate better understanding of chondrogenesis and optimization of cultivation conditions for cartilage tissue engineering.

Acknowledgments

The authors thank Robert Langer for his advice, Ivan Martin for help with image analysis, and John Barry and Rebecca Calzo for technical help. The research was supported by National Aeronautics and Space Administration (Grant NAG9-836).

Literature Cited

Bolis, S., C. J. Handley, and W. D. Comper, ''Passive Loss of Proteoglycan from Articular Cartilage Explants,'' *Biochim. Biophys. Acta*, **993**, 157 (1989).

Buckwalter, J. A., L. C. Rosenberg, and E. B. Hunziker, ''Articular Cartilage: Composition, Structure, Response to Injury and Methods of Facilitating Repair,'' *Articular Cartilage and Knee Joint Function: Basic Science and Arthroscopy*, J. W. Ewing, ed., Raven Press, New York, p. 19 (1990).

Buckwalter, J. A., and H. J. Mankin, ''Articular Cartilage Repair and Transplantation,'' *Arthritis Rheum.*, **41**, 1331 (1998).

Bursac, P. M., L. E. Freed, R. J. Biron, and G. Vunjak-Novakovic,

''Mass Transfer Studies of Tissue Engineered Cartilage,'' *Tiss. Eng.*, **2**, 141 (1996).
Buschmann, M. D., Y. A. Gluzband, A. J. Grodzinsky, J. H. Kimura, and E. B. Hunziker, ''Chondrocytes in Agarose Culture Synthesize a Mechanically Functional Extracellular Matrix,'' *J. Orthop. Res.*, **10**, 745 (1992).
Campbell, M. A., C. J. Handley, and S. E. D'Souza, ''Turnover of Proteoglycans in Articular-Cartilage Cultures,'' *Biochem. J.*, **259**, 21 (1989).
Comper, W. D., and R. P. W. Williams, ''Hydrodynamics of Concentrated Proteoglycan Solutions,'' *J. Biol. Chem.*, **262**, 13464 (1987).
Clark, C. C., B. S. Tolin, and C. T. Brighton, ''The Effect of Oxygen Tension on Proteoglycan Synthesis and Aggregation in Mammalian Growth Plate Chondrocytes,'' *J. Orthop. Res.*, **9**, 477 (1991).
Farndale, R. W., D. J. Buttle, and A. J. Barrett, ''Improved Quantitation and Discrimination of Sulphated Glycosoaminoglycans by the Use of Dimethylmethylene Blue,'' *Biochim. Biophys. Acta*, **883**, 173 (1986).
Freed, L. E., J. C. Marquis, A. Nohria, J. Emmanual, A. G. Mikos, and R. Langer, ''Neocartilage Formation in vitro and in vivo using Cells Cultured on Synthetic Biodegradable Polymers,'' *J. Biomed. Mat. Res.*, **27**, 11 (1993).
Freed, L. E., J. C. Marquis, G. Vunjak-Novakovic, J. Emmanual, and R. Langer, ''Composition of Cell-Polymer Cartilage Implants,'' *Biotech. Bioeng.*, **43**, 605 (1994a).
Freed, L. E., G. Vunjak-Novakovic, J. C. Marquis, and R. Langer, ''Kinetics of Chondrocyte Growth in Cell-Polymer Implants,'' *Biotech. Bioeng.*, **43**, 597 (1994b).
Freed, L. E., G. Vunjak-Novakovic, R. J. Biron, D. B. Eagles, D. C. Lesnoy, S. K. Barlow, and R. Langer, ''Biodegradable Polymer Scaffolds for Tissue Engineering,'' *Bio/Technology*, **12**, 689 (1994c).
Freed, L. E., and G. Vunjak-Novakovic, ''Cultivation of Cell-Polymer Tissue Constructs in Simulated Microgravity,'' *Biotech. Bioeng.*, **46**, 306 (1995).
Freed, L. E., R. Langer, I. Martin, N. R. Pellis, and G. Vunjak-Novakovic, ''Tissue Engineering of Cartilage in Space,'' *Proc. Natl. Acad. USA*, **94**, 13885 (1997).
Freed, L. E., A. P. Hollander, I. Martin, J. R. Barry, R. Langer, and G. Vunjak-Novakovic, ''Chondrogenesis in a Cell-Polymer-Bioreactor System,'' *Exp. Cell Res.*, **240**, 58 (1998).
Freed, L. E., I. Martin, and G. Vunjak-Novakovic, ''Frontiers in Tissue Engineering: in Vitro Modulation of Chondrogenesis,'' *Clin. Orthop. Rel. Res.*, 367S, S46 (1999).
Freed, L. E., and G. Vunjak-Novakovic, ''Tissue Engineering of Cartilage,'' *Biomedical Engineering Handbook*, J. D. Bronzino, ed., 2nd ed., CRC Press, Boca Raton, FL, 124 (2000a).
Freed, L. E., and G. Vunjak-Novakovic, ''Tissue Culture Bioreactors,'' *Principles of Tissue Engineering*, R. P. Lanza, R. Langer, and W. Chick, eds., 2nd ed., Academic Press, San Diego, CA, 143 (2000b).
Galban, C., and B. R. Locke, ''Analysis of Cell Growth in a Polymer Scaffold using a Moving Boundary Approach,'' *Biotechnol. Bioeng.*, **56**, 422 (1997).
Galban, C., and B. R. Locke, ''Analysis of Cell Growth Kinetics and Substrate Diffusion in a Polymer Scaffold,'' *Biotechnol. Bioeng.*, **65**, 121 (1999).
Hascall, V. C., J. D. Sandy, and C. J. Handley, ''Regulation of Proteoglycan Metabolism in Articular Cartilage,'' *Biology of the Synovial Joint*, C. W. Archer, ed., Ch 7, Harwood Academic Publishers, Amsterdam (1999).
Haselgrove, J. C., I. M. Shapiro, and S. F. Silverton, ''Computer Modeling of the Oxygen Supply and Demand of Cells of the Avian Growth Cartilage,'' *Am. J. Physiol.*, 265 (*Cell Physiol.*, 34), C497 (1993).
Hollander, A. P., T. F. Heathfield, C. Webber, Y. Iwata, R. Bourne, C. Rorabeck, and A. R. Poole, ''Increased Damage to type II Collagen in Osteoarthritic Articular Cartilage Detected by a New Immunoassay,'' *J. Clin. Invest.*, **93**, 1722 (1994).
Kim, Y. J., R. L. Sah, J. Y. H. Doong, and A. J. Grodzinsky, ''Fluorometric Assay of DNA in Cartilage Explants using Hoechst 33258,'' *Anal. Biochem.*, **174**, 168 (1988).
Kuettner, K. E., V. A. Memoli, B. U. Pauli, N. C. Wrobel, M. A. Thonar, and J. C. Daniel, ''Synthesis of Cartilage Matrix by Mammalian Chondrocytes in vitro: Maintenance of Collagen and Proteoglycan,'' *J. Cell. Bio.*, **93**, 751 (1982).
Langer, R., and J. P. Vacanti, ''Tissue Engineering,'' *Science*, 260, 920 (1993).
Neitzel, G. P., R. M. Nerem, A. Sambanis, M. K. Smith, T. M. Wick, J. B. Brown, C. Hunter, I. Jovanovic, P. Malaviya, S. Saini, and S. Tan, ''Cell Function and Tissue Growth in Bioreactors: Fluid-Mechanical and Chemical Environments,'' *J. Japan Microgr. Appl.*, 15 (suppl. II), 602 (1998).
von Rosenberg, D. U., *Methods for the Numerical Solution of Partial Differential Equations*, American Elsevier Publishing Company, Inc., New York (1969).
Marcus, R. E., ''The Effect of Low Oxygen Concentration on Growth, Glycolysis and Sulfate Incorporation by Articular Chondrocytes in Monolayer Culture,'' *Arthritis Rheum.*, **16**, 646 (1973).
Maroudas, A., ''Physicochemical Properties of Articular Cartilage,'' *Adult Articular Cartilage*, M. A. R. Freeman, ed., 2nd ed., Chap. 4, Pitman Medical, London (1979).
Martin, I., B. Obradovic, L. E. Freed, and G. Vunjak-Novakovic, ''A Method for Quantitative Analysis of Glycosaminoglycan Distribution in Cultured Natural and Engineering Cartilage,'' *Ann. Biomed. Eng.*, **27**, 1 (1999).
Obradovic, B., L. E. Freed, R. Langer, and G. Vunjak-Novakovic, ''Bioreactor Studies of Natural and Engineered Cartilage Metabolism,'' *Proc. of the Topical Conf. on Biomaterials, Carriers for Drug Delivery, and Scaffolds for Tissue Engineering*, N. A. Peppas, D. J. Mooney, A. G. Mikos, and L. Brannon-Peppas, eds., AIChE, New York, p. 335 (1997).
Obradovic, B., R. L. Carrier, G. Vunjak-Novakovic, and L. E. Freed, ''Gas Exchange is Essential for Bioreactor Cultivation of Tissue Engineered Cartilage,'' *Biotech. Bioeng.*, **63**, 197 (1999).
O'Driscoll, S. W., J. S. Fitzsimmons, and C. N. Commisso, ''Role of Oxygen Tension during Cartilage Formation by Periosteum,'' *J. Orthop. Res.*, **15**, 682 (1997).
Scott, J. E., ''Oxygen and the Connective Tissues,'' *TIBS*, **17**, 340 (1992).
Shapiro, I. M., T. Tokuoka, and S. F. Silverton, ''Energy Metabolism in Cartilage,'' *Cartilage: Molecular Aspects*, B. Hal and S. Newman, eds., Chap. 3, CRC Press, Boca Raton, FL (1991).
Vunjak-Novakovic, G., L. E. Freed, R. J. Biron, and R. Langer, ''Effects of Mixing on the Composition and Morphology of Tissue-Engineered Cartilage,'' *AIChE J.*, **42**, 850 (1996).
Vunjak-Novakovic, G., B. Obradovic, I. Martin, P. M. Bursac, R. Langer, and L. E. Freed, ''Dynamic Cell Seeding of Polymer Scaffolds for Cartilage Tissue Engineering,'' *Biotechnol. Prog.*, **14**, 193 (1998).
Vunjak-Novakovic, G., I. Martin, B. Obradovic, S. Treppo, A. J. Grodzinsky, and L. E. Freed, ''Bioreactor Cultivation Conditions Modulate the Composition and Mechanical Properties of Tissue-Engineered Cartilage,'' *J. Orthop. Res.*, **17**, 130 (1999).
Ysart, G. E., and R. M. Mason, ''Responses of Articular Cartilage Explant Cultures to Different Oxygen Tensions,'' *Biochim. Biophys. Acta*, **1221**, 15 (1994).

Manuscript received Sept. 29, 1999, and revision received Apr. 11, 2000.